Supporting Information

Diameter Dependent Electron Transfer Kinetics in Semiconductor-Enzyme complexes

Katherine A. Brown,[1] Qing Song,[2] David W. Mulder,[1] and Paul W. King[1*]

[1]Biosciences Center, National Renewable Energy Laboratory, Golden CO 80401
[2]IBM Almaden Research Center, San Jose, CA, 95120, United States

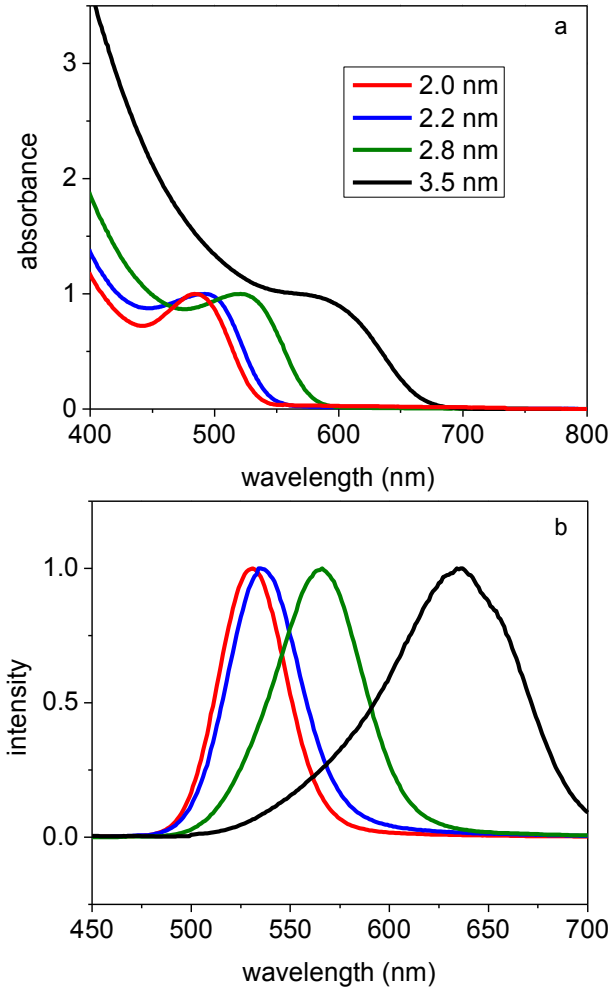

Figure S1. Optical properties of CdTe samples. (a) Normalized UV-Vis absorbance spectra, and (b) normalized photoluminescence spectra of different diameters of CdTe nanoparticles in Tris-HCl buffer, pH 7.

Method for Determining CdTe Diameter Values. The diameter for each CdTe sample (*d*) was determined from the first excited state 1S3/2(h)→1S(e) transition peak wavelength (λ) as described in Yu *et al*.[1]

d (nm) = $(9.8127 \times 10^{-7})\lambda^3 - (1.7147 \times 10\text{-}3)\lambda^2 + (1.0064)\lambda - 194.84$

Fluorescence decay Fits. The fluorescence decays were fit to triple exponential kinetic function,

$$y = y_0 + A_1 e^{-t/\tau 1} + A_2 e^{-t/\tau 2} + A_3 e^{-t/\tau 3}$$

which provided the best quality fit as determined by chi-squared test (Table S1). The average fluorescent lifetime for each sample was calculated using:

$$\tau_{\text{obs}} = \sum A_i \tau_1^2 \Big/ \sum A_i \tau_i$$

Table S1. Chi-squared (χ^2) values for double, triple and quadruple exponential fits of CdTe fluorescence decays.

CdTe Diameter (nm)	Double exponential χ^2	Triple exponential χ^2	Quadruple exponential χ^2
2.0	8.4	1.9	1.9
2.2	5.7	2.1	2.0
2.8	5.7	2.1	2.1
3.4	12.5	1.8	1.7

Table S2. CdTe fluorescent lifetimes over a range of CdTe:CaI molar ratios.

CdTe:CaI molar ratio	**2.0 nm CdTe τ_{obs} (ns)**	**2.2 nm CdTe τ_{obs} (ns)**	**2.8 nm CdTe τ_{obs} (ns)**	**3.5 nm CdTe τ_{obs} (ns)**
1:0	40 ± 2	42 ± 2	43 ± 1	46 ± 2
10:1	37 ± 3	38 ± 2	38 ± 2	38 ± 2
5:1	35 ± 2	37 ± 2	35 ± 2	31 ± 3
2:1	35 ± 3	36 ± 1	32 ± 2	29 ± 2
1:1	32 ± 2	33 ± 2	29 ± 2	26 ± 1
1:2	27 ± 2	29 ± 3	26 ± 2	24 ± 2
1:4	23 ± 2	27 ± 2	24 ± 1	19 ± 3
1:8	22 ± 1	20 ± 2	19 ± 2	17 ± 1
1:16	21 ± 1	18 ± 2	16 ± 1	14 ± 2

Table S3. **Equilibrium CdTe-CaI complex concentration present in solution.**

CaI:CdTe molar ratio	[CdTe-CaI] (µM) 2.0 nm CdTe[a]	[CdTe-CaI] (µM) 2.2 nm CdTe[b]	[CdTe-CaI] (µM) 2.8 nm CdTe[c]	[CdTe-CaI] (µM) 3.5 nm CdTe[d]
1:16	0.4	0.4	0.3	0.3
1:8	0.7	0.6	0.6	0.7
1:4	1.5	1.4	1.3	1.5
1:2	2.9	2.7	2.5	3.0
1:1	5.9	5.5	5.0	5.9
2:1	11.7	11.0	10.1	11.9
5:1	29.3	27.4	25.4	29.7
10:1	58.5	54.9	50.7	59.4

[a][2.0 nm CdTe] = 3.67 µM

[b][2.2 nm CdTe] = 2.8 µM

[c][2.8 nm CdTe] = 2.0 µM

[d][3.5 nm CdTe] = 1.2 µM

Method for Determining CdTe Nanoparticle Reduction Potentials. Mixtures of 0.8 µM CdTe nanoparticles and 16 mM methyl viologen (MV, Sigma) were combined under an anaerobic N_2 atmosphere in 50 mM Tris-HCl buffers of varying pH (2, 2.5, 3, 3.4, 4 and 4.5). Samples were illuminated for 10 min with the same 405 nm LED light source used in H_2 production experiments (2500 µmol photon m^{-2} s^{-1}). Absorbance spectra were collected on a Beckman DU800 and the concentration of reduced MV was determined by absorbance at 606 nm (A_{606}), as shown in Figure S2 for 2.0 nm CdTe. The potential of the conduction band electrons for each diameter of CdTe at standard reaction conditions were determined by extrapolation to pH 7 using the Nernst equation as previously described.[2,3]

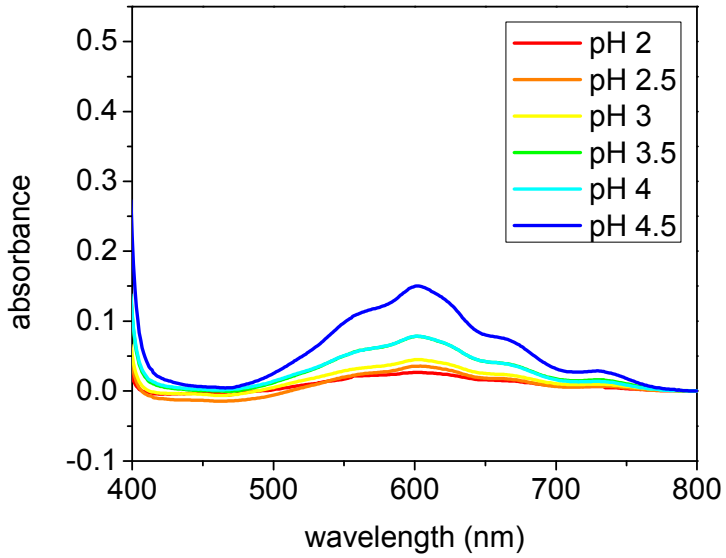

Figure S2. Difference spectra of MV reduction by 2.0 nm CdTe after 10 min. Illumination with 405 nm light in various pH buffers. UV-visible spectra were collected before and after illumination. The A_{606} peak was not observed in solutions prior to illumination. Difference spectra were used for excited state conduction band-edge potential determination to remove CdTe absorbance signal from MV absorbance.

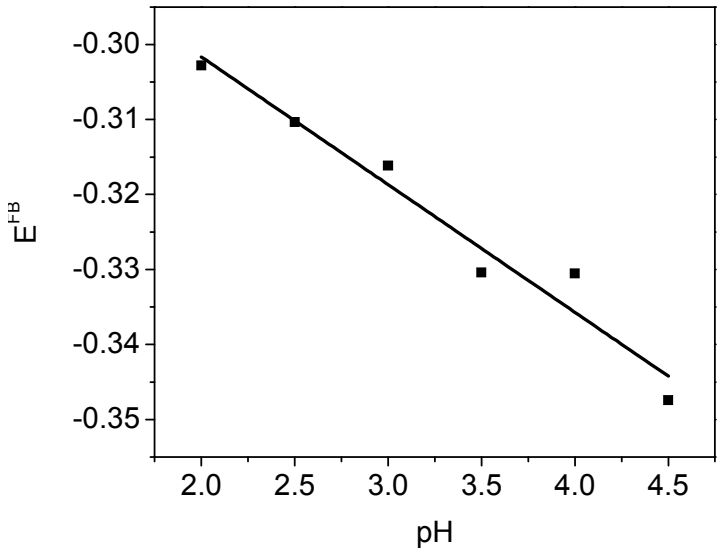

Figure S3. pH dependence of 2.0 nm CdTe flat band potential. Nanoparticle potential was calculated from the theoretical E^{FB} at pH 0 using the Nernst equation and data plotted in Figure S2 as previously described.[2,3]

Table S4. CdTe reduction potentials and ΔG_{ET} values at pH 7.

CdTe diameter (nm)	[a]Conduction band potential pH 7 (mV vs NHE)	[b]ΔG_{ET} Redox pH 7 (mV)
2.0	-670 ± 10	250
2.2	-600 ± 20	180
2.8	-490 ± 20	70
3.5	-450 ± 20	30

[a]Measured by MV assay of E_{CdTe}.[2,3]
[b]Calculated as $\Delta G_{ET}=(E_{CdTe} - E_{Cal})$, at pH 7 (vs. NHE).

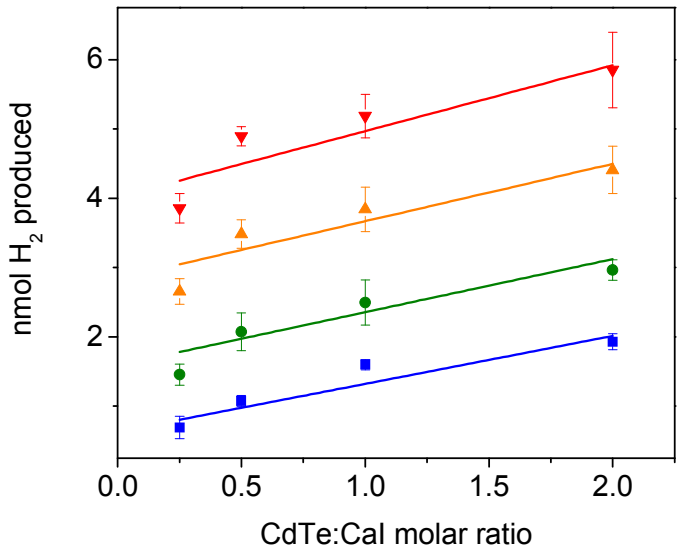

Figure S4. H_2 production by CdTe-CaI complexes at 1:0.5, 1:1, 1:2 and 1:4 CdTe:CaI molar ratios for 2.0 nm (blue squares), 2.2 nm (green circles), 2.8 nm (orange triangles) and 3.5 nm (red diamonds) CdTe. Lines represent linear fits. Samples illuminated for 5 min with 405 nm light (2500 µmol photon m-2 s-1) with 100 mM AA. CdTe concentration normalized to A_{405} = 0.01 ([CdTe] 2.0 nm, 0.31 µM; 2.2 nm, 0.28 µM; 2.8 nm, 0.13 µM; and 3.5 nm, 0.073 µM).

Table S5. Quantum yield of H_2 (QY_{H2}) production for 1:2 CaI:CdTe molar ratio for each CdTe diameter.

CdTe diameter (nm)	[a]QY_{H2} (%)
2.0	1.7 ± 0.4
2.2	5.0 ± 0.6
2.8	9.1 ± 1.1
3.5	12.2 ± 1.0

[a] $QY_{H2} = \frac{mole\ H_2\ produced}{2 * absorbed\ photons}$

CdTe-CaI Binding Models

From the crystal structure of CpI we approximate the dimensions of CaI were modeled as follows:

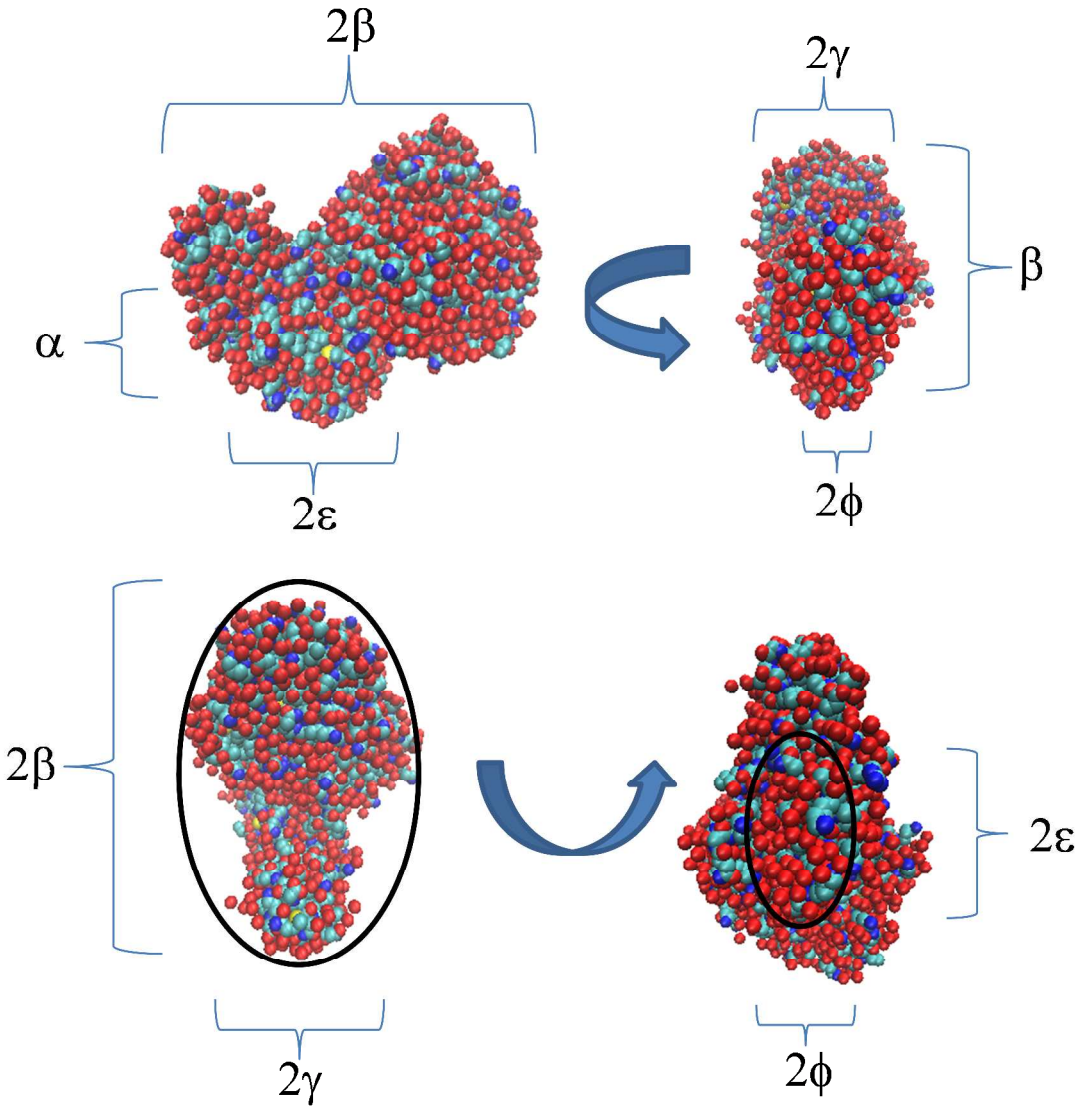

α = 4 nm β = 1.21 nmγ = 2 nm ε = 2.25 nm ϕ = 1.125 nm

Figure S5. Physical dimensions of [FeFe]-hydrogenase CaI based on homology structural model to CpI PDB ID 1feh.[4]

Cone binding model. CaI is modelled as a truncated elliptical cone (Figure S6a). The interaction between an elliptical cone and the surface of a sphere with radius r can be defined by the elliptical footprint as shown in green in Figure S6b and S6c. The angle of deflection between the extension of the cone and the center of the sphere (σ_1 and σ_1) can be used to define the footprint (Figure S7). The axes of the footprint ellipse (x1 and x2) can be calculated using basic geometry.

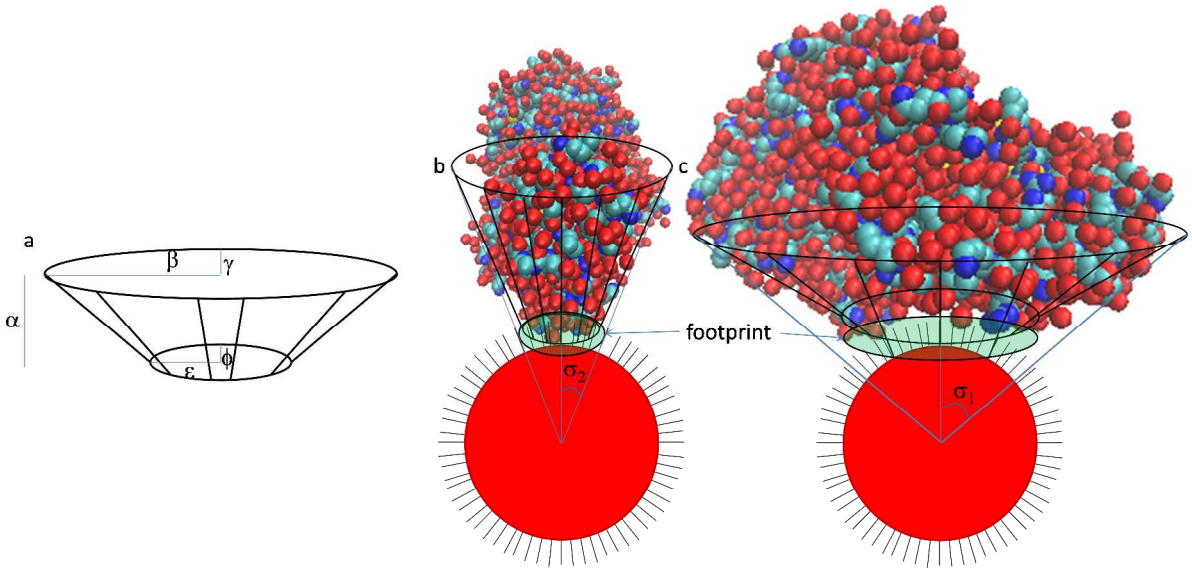

Figure S6. Cone model of CaI binding on CdTe.

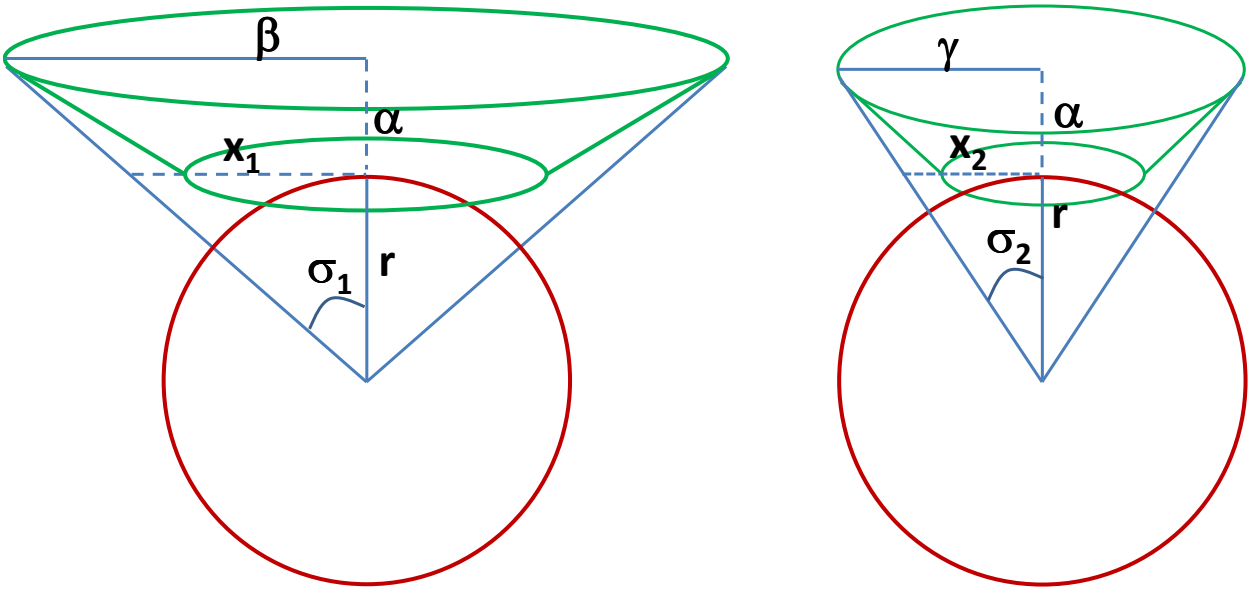

$$\tan\sigma_1 = \frac{\beta}{\alpha+r} \qquad \tan\sigma_2 = \frac{\gamma}{\alpha+r}$$

$$x_1 = r\tan\sigma_1 \qquad x_2 = r\tan\sigma_2$$

$$x_1 = \frac{r\beta}{\alpha+r} \qquad x_1 = \frac{r\gamma}{\alpha+r}$$

Figure S7. Cone model geometry of CaI binding to CdTe.

Table S6. Parameters and values for angles of deflection and footprint dimensions for Cone binding model.

CdTe diameter (nm)	r (nm)	r+α (nm)	σ_1 (radian)	σ_2 (radian)	x_1 (nm)	x_2 (nm)	Footprint area (nm^2)	CdTe surface area (nm^2)	CaI binding sites
2.0	1.5	2.71	0.98	0.69	2.2	1.2	8.7	28.3	3.3
2.2	1.6	2.81	0.96	0.68	2.3	1.3	9.2	32.2	3.5
2.8	1.9	3.11	0.91	0.63	2.4	1.4	10.6	45.4	4.3
3.5	2.25	3.46	0.86	0.58	2.6	1.5	12.0	63.6	5.3

Ellipsoid binding model. Using the largest dimensions of CaI (2α, β and γ) CaI is modeled as an ellipsoid. The volume around CdTe available to CaI is defined as a sphere with radius R = r + 2a. For each CdTe diameter, we defined a binding sphere around the nanoparticle with a radius R = r + 2α, where r is the nanoparticle radius and α is the vertical dimension of CaI shown in Figure 3b. The CaI ellipsoid volume is 45.6 nm^2 for all CdTe diameters, and the volume available for CaI binding (V_B) was defined by the equation:

$$V_B = \frac{4}{3}\pi[(r + 2\alpha)^3 - r^3]$$

Table S7. Parameters and binding site values for Ellipsoid binding model.

CdTe diameter (nm)	r (nm)	r+α (nm)	V_B (nm^3)	CaI binding sites
2.0	1.5	2.71	238.2	5.2
2.2	1.6	2.81	255.0	5.6
2.8	1.9	3.11	309.0	6.8
3.5	2.25	3.46	378.9	8.3

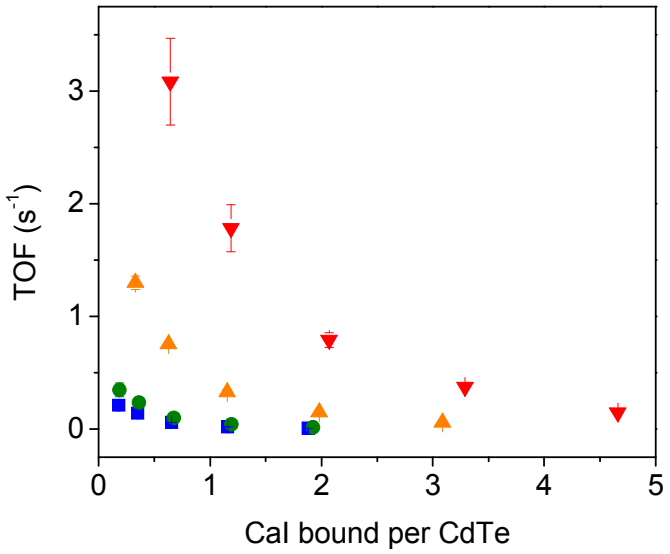

Figure S8. CaI TOF in CdTe-CaI complexes. TOF at 4:1, 1:1, 1:1, 2:1 and 4:1 CaI:CdTe molar ratios as a function the average CaI bound per CdTe binding site (CaI_B) calculated from the Ellipsoid binding model. Samples illuminated for 5 min with 405 nm light (2500 µmol photon m^{-2} s^{-1}) with 100 mM AA. CdTe concentration normalized to A_{405} = 0.01 ([CdTe] 2.0 nm, 0.31 µM; 2.2 nm, 0.28 µM; 2.8 nm, 0.13 µM; and 3.5 nm, 0.073 µM).

Table S8. CdTe recombination rates.

CdTe diameter (nm)	k_{CdTe} (s^{-1})
2.0	2.48×10^7
2.2	2.35×10^7
2.8	2.31×10^7
3.5	2.17×10^7

References

(1) Yu, W. W.; Qu, L.; Guo, W.; Peng, X. Experimental Determination of the Extinction Coefficient of CdTe, CdSe, and CdS Nanocrystals. *Chem. Mater.* 2003, 15, 2854-2860.

(2) Brown, K. A.; Dayal, S.; Ai, X.; Rumbles, G.; King, P. W. Controlled Assembly of Hydrogenase-CdTe Nanocrystal Hybrids for Solar Hydrogen Production. *J. Am. Chem. Soc.* 2010, 132, 9672-9680.

(3) Brown, K. A.; Wilker, M. B.; Boehm, M.; Dukovic, G.; King, P. W. Characterization of Photochemical Processes for H2 Production by CdS Nanorod–[FeFe] Hydrogenase Complexes. *J. Am. Chem. Soc.* 2012, 134, 5627-5636.

(4) Peters, J. W.; Lanzilotta, W. N.; Lemon, B. J.; Seefeldt, L. C. X-Ray Crystal Structure of the Fe-Only Hydrogenase (CpI) from *Clostridium pasteurianum* to 1.8 Angstrom Resolution. *Science* 1998, 282, 1853-1858.